



**HAL**  
open science

## Plastic deformation of bunsenite (NiO) at temperatures below 1 050 °C

F. Guiberteau, A. Donminguez-Rodriguez, M. Spendel, J. Castaing

► **To cite this version:**

F. Guiberteau, A. Donminguez-Rodriguez, M. Spendel, J. Castaing. Plastic deformation of bunsenite (NiO) at temperatures below 1 050 °C. *Revue de Physique Appliquée*, 1986, 21 (2), pp.87-92. 10.1051/rphysap:0198600210208700 . jpa-00245426

**HAL Id: jpa-00245426**

**<https://hal.science/jpa-00245426>**

Submitted on 4 Feb 2008

**HAL** is a multi-disciplinary open access archive for the deposit and dissemination of scientific research documents, whether they are published or not. The documents may come from teaching and research institutions in France or abroad, or from public or private research centers.

L'archive ouverte pluridisciplinaire **HAL**, est destinée au dépôt et à la diffusion de documents scientifiques de niveau recherche, publiés ou non, émanant des établissements d'enseignement et de recherche français ou étrangers, des laboratoires publics ou privés.

Classification  
 Physics Abstracts  
 62.20F — 81.40L

## Plastic deformation of bunsenite (NiO) at temperatures below 1 050 °C

F. Guiberteau (\*), A. Donminguez-Rodriguez

Departamento de Optica, Facultad de Fisica, Apartado 1065, Sevilla, Spain

M. Spendel and J. Castaing

Laboratoire de Physique des Matériaux, C.N.R.S.,  
 1, Place A. Briand, 92195 Meudon Pal Cedex, France

(Reçu le 17 septembre 1984, révisé les 12 avril et 13 août 1985, accepté le 12 novembre 1985)

**Résumé.** — Des essais de compression à vitesse constante ( $\dot{\epsilon} \sim 7 \times 10^{-5} \text{ s}^{-1}$ ) ont été réalisés sur des monocristaux de NiO selon les directions  $\langle 100 \rangle$  et  $\langle 111 \rangle$ . La contrainte d'écoulement plastique, le taux de consolidation et les paramètres d'activation thermique ont été déterminés entre 77 K et 1 323 K. La contrainte à la limite élastique pour des essais selon  $\langle 100 \rangle$  montre une anomalie à la température de Néel bien moindre que celle publiée précédemment [3, 5]. L'anisotropie plastique est comparée à celles de quelques composés ioniques, et les mécanismes de durcissement sont discutés sur la base des données mécaniques.

**Abstract.** — Constant strain rate compression tests along  $\langle 100 \rangle$  and  $\langle 111 \rangle$  have been performed on NiO single crystals ( $\dot{\epsilon} \sim 7 \times 10^{-5} \text{ s}^{-1}$ ). Yield stresses, work hardening rates and thermal activation parameters have been measured between 77 K and 1 323 K. The flow-stress for samples compressed along  $\langle 100 \rangle$  shows an anomaly at the Néel temperature much smaller than the one previously published [3, 5]. The plastic anisotropy is compared to other ionic compounds and the hardening mechanism are discussed based on mechanical data.

### 1. Introduction.

The properties of transition metal oxides have been the subject of many investigations [1]. However, their mechanical properties have not received much attention; they are important not only in some applications, e.g. high temperature corrosion, but in the understanding of the elementary processes of deformation of materials.

In the past, we have studied the plasticity of nickel oxide at high temperature [2], as well as at low temperature [3] where it shows extensive plasticity, like ionic crystals sharing the same rock-salt crystal structure [4]. NiO single crystals were tested in compression along  $\langle 100 \rangle$  at temperatures  $T$  as low as 201 K [3]; we have performed tests down to 77 K ( $0.03 T_M$  where  $T_M = \text{melting temperature} = 2 257 \text{ K}$ ).

NiO plasticity exhibits some peculiarities; (i) impurities can harden or soften NiO [3, 5], (ii) the anti-

ferromagnetic ordering below  $T_N = 520 \text{ K}$  (Néel temperature), was associated with a discontinuity in the flow stress  $\sigma_f$ - $T$  curve [3, 5] much larger than in CoO [6]. We have made a new study, with an improved thermal control, of the plastic behaviour around  $T_N$ , which is not in agreement with the previous observations.

There are a few transmission electron microscopy observations of NiO which give a few insights on its plastic deformation [7, 8]. Fuertes [8] found  $\sigma_f$  values different from those previously published [3], in particular at  $T = 773 \text{ K}$ ; this was tentatively attributed to differences in point defect configurations [8]; our new data are closer to those of Fuertes [8] than the previous ones [3].

This study was not restricted to these new results. We have compared the plastic behaviour of NiO single crystals grown by the arc image furnace and the Verneuil techniques. We have also performed compression tests along  $\langle 111 \rangle$  which give no shear stress on  $\{110\} \langle 110 \rangle$ , the usual slip system in rocksalt structure crystals. This gives a first account of the plastic anisotropy of nickel oxide.

(\*) Permanent address : Dpto. Electricidad y Electronica, Facultad de Ciencias, Universidad de Extremadura, Badajoz.

## 2. Experimental techniques.

**2.1 SAMPLE PREPARATION AND CHARACTERIZATION.** — Two crystal growth techniques have been used to make NiO single crystals. They both start with the same high purity Johnson-Matthey powder. The first one is the zone melted technique in an arc image furnace; crystals in our previous studies [3, 5] have all been prepared along this way, which is likely to give materials of higher purity than the second technique, viz. the Verneuil process. However, crystallographic quality of Verneuil crystals seems better. This has been checked by X-ray Laue diffraction and by the aspect of the  $\{100\}$  planes after cleavage. More details on the crystals can be found in the paper of Dubois *et al.* [9]. Specimens for compression were parallelepipeds of sizes between  $2 \times 2 \times 5 \text{ mm}^3$  and  $3 \times 3 \times 5 \text{ mm}^3$ . Their orientation was determined by cleavage or by X-ray Laue diffraction. When the stress  $\sigma$  was applied along  $\langle 100 \rangle$ , all faces were of  $\{100\}$  type; for  $\sigma$  along  $\langle 111 \rangle$ , the lateral faces were of  $\{110\}$  and  $\{11\bar{2}\}$  type. They were generally as-cleaved or as-cut with a low speed diamond saw. All specimens were annealed in air at  $1200^\circ\text{C}$  for more than two days and air quenched to room temperature prior to mechanical testing.

After deformation, a few specimens were optically examined to check for slip systems, either by observing steps, or by chemical etch-pitting on  $(100)$  cleaved faces (9 vol  $\text{H}_3\text{PO}_4$  + 1 vol  $\text{HNO}_3$  at  $140^\circ\text{C}$  during 15 min or  $\text{HNO}_3$  at  $105^\circ\text{C}$  during 30 min).

**2.2 MECHANICAL TESTING.** — Compression at a constant cross-head velocity (20  $\mu\text{m}/\text{min}$ ; strain rate  $\dot{\epsilon} \sim 7 \times 10^{-5} \text{ s}^{-1}$ ) have been performed in an Instron machine. For tests at  $T < 400^\circ\text{C}$ , samples are in a liquid: oil above  $0^\circ\text{C}$ , acetone and liquid nitrogen below  $0^\circ\text{C}$  [6]. By immersing a sample in oil at room temperature during a test, the plastic properties were not modified. Above  $400^\circ\text{C}$ , the tests were performed in air in the set-up used in previous works [3, 5].

The results are displayed using engineering stress  $\sigma$  and strain  $\epsilon$ . Activation volumes  $V$  have been measured either by relaxation tests or by strain rate changes; the data analysis was the same as in our previous work [3].

## 3. Results.

### 3.1 COMPRESSION ALONG $\langle 100 \rangle$ .

**3.1.1 Stress strain ( $\sigma$ - $\epsilon$ ) behaviour.** — NiO single crystals have been deformed above 77 K. At the lower limit of  $T$ , only small plastic strains were achieved without failure of the samples; the image furnace crystals were harder and more brittle than the Verneuil ones (Fig. 1).

The change from elastic to plastic deformation is generally gradual (Fig. 1); this may be due either to the non-uniaxial stress tensor in compression test

or to the activation of multiple slip at the onset of plasticity. Around  $300$ - $400^\circ\text{C}$ , the work hardening rate is very large. Sometimes,  $\sigma$ - $\epsilon$  curves having a rather parabolic shape were observed; this behaviour has been reported by Fuertes [8]. Around room temperature, the yield stress is generally followed by various stages (Fig. 1) with different work hardening rates. Above  $600^\circ\text{C}$ , a quasi steady state is reached at yielding and deformation as large as 30% can be reached.

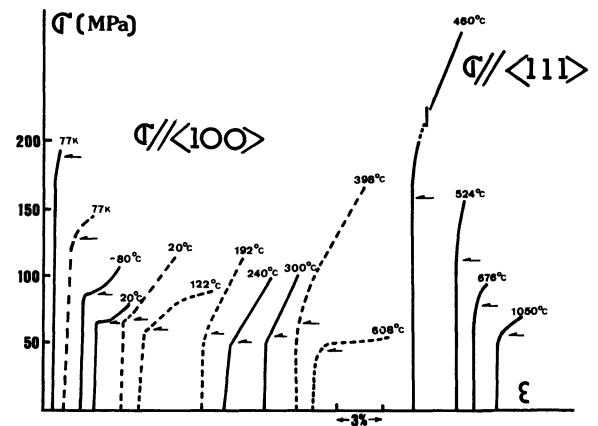


Fig. 1. — Engineering stress  $\sigma$  versus engineering strain  $\epsilon$  for NiO deformed by constant strain rate compression at various temperatures.  $\dot{\epsilon} \sim 7 \times 10^{-5} \text{ s}^{-1}$ . The arrow indicates the  $\sigma_{0.2}$  values for figure 2. Solid curves correspond to arc image sample (I), while dashed curves correspond to Verneuil samples (V).

**3.1.2 Yield stress and work hardening.** — We characterize the onset of plasticity in NiO by  $\sigma_{0.2}$ , the proof stress for a strain of 0.2% and the work hardening rate by  $\theta = d\sigma/d\epsilon$ . Their values are shown in figures 2 and 3. Below  $500^\circ\text{C}$ , the  $\sigma_{0.2}$  values are larger than those of our previous work (Fig. 2). Because of the large number of determinations, the statistical weight of the present data is much greater than that of our previous data [3]. Below the Néel temperature  $T_N$ , there is a plateau in the  $\sigma_{0.2}$ - $T$  curve (Fig. 2).

At room temperature,  $\sigma_{0.2}$  values are scattered as shown in the inset of figure 2 where are displayed data for various kinds of specimens cut in the two types of crystals. In addition to specimens prepared along the standard procedure described in section 2.1, we have tested six specimens named « J » (Fig. 2), either made out of uncontrolled quality crystals, or having non-standard dimensions; they are stronger than all other specimens and their  $\sigma_{0.2}$  values were discarded. In order to check for the influence of surface preparation, two Verneuil crystal specimens were mechanically polished; their  $\sigma_{0.2}$  values were slightly larger than for standard specimens (compare  $V_p$  and  $V$  in Fig. 2), the difference is too small to draw any conclusion.

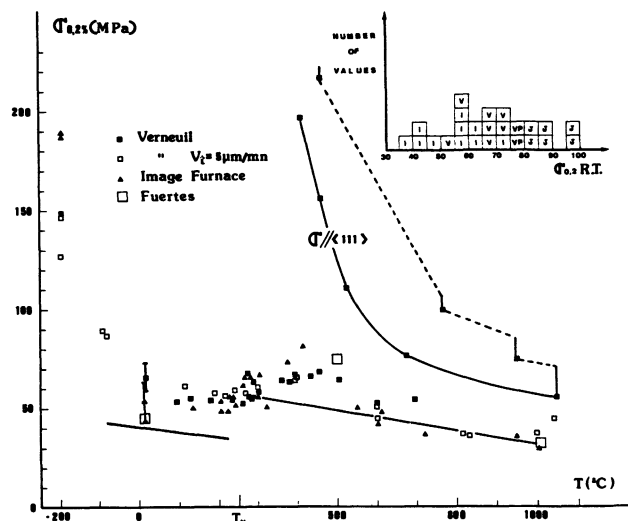


Fig. 2. — Variation with temperature of the engineering stress, at  $\epsilon = 0.2\%$ ,  $\sigma_{0.2}$  for  $\sigma$  parallel to  $\langle 111 \rangle$  and  $\langle 100 \rangle$ . The results were generally obtained for a cross head velocity of  $20 \mu\text{m}/\text{mn}$  with crystals made in the arc image furnace (I) or by the Verneuil technique (V). We have also plotted the results of A. Dominguez-Rodriguez [3] (straight line) and of M. Fuertes [8] for  $\sigma$  parallel to  $\langle 100 \rangle$ . The upper right insert shows the scatter of the room temperature values of  $\sigma_{0.2}$  for  $\sigma$  parallel to  $\langle 100 \rangle$ .

For the arc image crystals (I), we find, at room temperature, for  $\sigma_{0.2}$  a value of  $56 \pm 10$  MPa (10 values) smaller than for Verneuil crystals  $65 \pm 7$  MPa (7 values). These values are larger than the one of Fuertes [8] (Fig. 2), who has only a few determinations. At  $500^\circ\text{C}$ , Fuertes [8] finds a value slightly above ours (Fig. 2). To understand the large scatter of  $\sigma_{0.2}$  values (Fig. 2), a detailed study of the specimen microstructures (impurities, subboundaries...) is required. It is out of our reach. The scatter explains the discrepancies between data of authors who generally performed a limited number of tests.

The work hardening rates determined in the linear ranges of the  $\sigma$ - $\epsilon$  curves are shown in figure 3. They are rather scattered. This, probably, comes from the variable number of  $\{110\}$  slip planes which are activated during plastic flow; for one or two planes, we expect small  $\theta$  values, while for three or four planes, we expect large  $\theta$  values. Several stages are sometimes observed with varying hardening rates. Occasionally, we obtained an easy glide at low temperature (see Fig. 1, at  $20^\circ\text{C}$ ). All the values have been reported in figure 3. There is a trend for a maximum at  $T_N$  and a quick decrease at about  $500^\circ\text{C}$ . These observations are consistent with our previous ones [3].

Fuertes found  $\theta = 610$  and  $1140$  MPa at room temperature (two stages) and  $920 < \theta < 1500$  MPa at  $T = 500^\circ\text{C}$  (parabolic  $\sigma$ - $\epsilon$  curves) [8] in agreement with our data of figure 3.

**3.1.3 Thermal activation parameters.** — We have determined the activation volume  $V$  from stress relaxation tests. The results are very similar to those

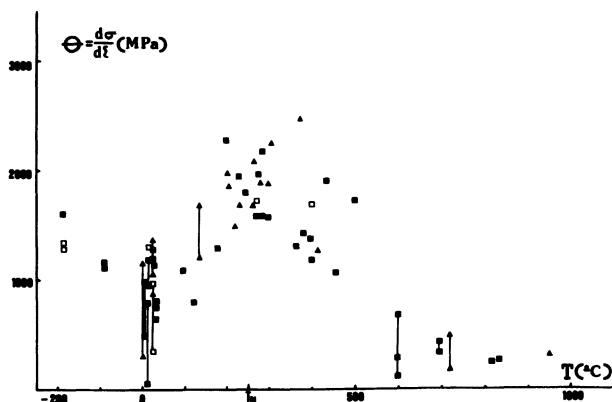


Fig. 3. — Variation of the work-hardening rate  $\theta$  with temperature. We use the same symbols as for figure 2. The vertical bars correspond to  $\sigma$ - $\epsilon$  curves with several stages with different work-hardening rates.  $\theta$  values are measured for  $\epsilon$  between 3 and 5 %.

found earlier [3, 5]. We have observed a decrease of  $V$  for increasing  $\sigma$  when deformation proceeds at  $T > 150^\circ\text{C}$ , with  $V$  in the range  $500 b^3$ - $1000 b^3$  ( $b^3 = 25.9 \times 10^{-30} \text{ m}^3$ ). At room temperature and below,  $V$  is insensitive to strain, with values of a few  $100 b^3$ , down to a few  $10 b^3$  at  $77 \text{ K}$ . There is no visible difference between image furnace and Verneuil grown crystals.

**3.2 COMPRESSION ALONG  $\langle 111 \rangle$ .** — In order to have some idea of the plastic anisotropy i.e. of the case for dislocation to slip in planes different from the usual  $\{110\}$ , we have stressed NiO Verneuil crystals along  $\langle 111 \rangle$ . For this orientation, the Schmid factor is zero for all the  $\{101\} \langle 101 \rangle$  slip systems and it is 0.47 for  $\{100\} \langle 011 \rangle$ .

We have performed five tests. At  $412^\circ\text{C}$ , no macroscopic plasticity was observed for  $\sigma = 286$  MPa. At  $460^\circ\text{C}$ , a strain of 3 % was reached (Fig. 1), with a final stress of 258 MPa. The flow stress is very sensitive to temperature for  $T < 600^\circ\text{C}$  (Fig. 2). A specimen was deformed at  $1050^\circ\text{C}$  and then cooled and strained at  $950^\circ\text{C}$ ,  $766^\circ\text{C}$  and  $460^\circ\text{C}$ ; the flow stresses are represented in figure 2 and related by a dashed line. For  $T > 600^\circ\text{C}$ ,  $\sigma_{0.2}$  shows similar variations with  $T$  for  $\sigma$  along  $\langle 111 \rangle$  and  $\langle 100 \rangle$  (Fig. 2). At  $1050^\circ\text{C}$ , the work hardening rate is somewhat higher for  $\sigma$  along  $\langle 111 \rangle$  than for  $\sigma$  along  $\langle 100 \rangle$  (Figs. 1 and 3); in addition the flow is unstable with serrations 2 MPa in amplitude, which could be due to Portevin Le Chatelier effect [10]. The plastic anisotropy can be summarized by the ratio of  $\sigma_{0.2}$  for  $\langle 111 \rangle$  direction over  $\langle 100 \rangle$  which is about 1.8 for  $600 < T < 1050^\circ\text{C}$ ; it increases sharply below  $600^\circ\text{C}$ .

We have determined the activation volume  $V$  by stress relaxation in a few cases finding that  $V/b^3 = 730$  at  $676^\circ\text{C}$  ( $\sigma = 89$  MPa), 90 at  $530^\circ\text{C}$  ( $\sigma = 170$  MPa) and 150 at  $460^\circ\text{C}$  ( $\sigma = 258$  MPa). These values would

fall within the ones for  $\sigma$  along  $\langle 100 \rangle$  suggesting similar mechanisms to control the glide of dislocations for both orientations.

#### 4. Discussion.

**4.1 MECHANICAL DATA.** — Yield stresses and work hardening rates measured for NiO single crystals show a fairly large scatter, with discrepancies between the various studies (Figs. 2 and 3). This situation is not worse than the one in other crystals e.g. in LiF, NaCl and MgO, the data for yield stresses are spread on almost a decade [4]. For NiO standard specimens, at room temperature,  $\sigma_{0.2}$  values for I and V crystals largely overlap (Fig. 2).

The difference in hardness of V and I crystals is not straightforward to explain since at 77 K I specimens are harder than V specimens, the reverse being observed at room temperature. At higher temperatures, there is no clear difference between the two kinds (Fig. 2). Speculations based on crystal perfection (impurities, boundaries, initial dislocation density...) leading to hardening or softening of the specimens, can give an account for these observations; they are not worthwhile in the absence of a systematic study.

**4.2 SLIP SYSTEM.** — We have examined by optical microscopy the slip systems that have been activated. For  $\sigma$  along  $\langle 100 \rangle$  at room temperature, we have studied 7 specimens, examining two orthogonal faces. We found the usual  $\{110\} \langle 110 \rangle$  slip systems (Fig. 4) in agreement with previous observations [3] and with T.E.M. studies [7, 8]. The etch pits reveal lines at 45° to the stress axis, which correspond to

the emergence of edge dislocations, screws are not etched. Four glide systems have the same Schmid factor and can be activated. In one case only, we had two orthogonal planes all over the specimen (Fig. 4). For other specimens, we found the four systems which have been activated by orthogonal pairs in different places.

There is no substantial change concerning the observations of glide bands made at various temperatures. At 77 K, only very thin bands were seen, but the specimens were only strained to  $\varepsilon = 0.5\%$ . At 300 °C, the specimens are covered with pits in a similar way to figure 4. We have annealed deformed specimens at 1 200 °C in air for a few days to estimate the recovery. No etch pits could be revealed after that. Moreover, at room temperature, these annealed specimens recovered their initial mechanical properties (4 tests). This proves that the anneal is sufficient to eliminate a large fraction of the dislocations introduced by deformation at room temperature.

The slip lines for  $\sigma$  along  $\langle 111 \rangle$  were short and wavy (Fig. 5), similar to what has been observed for NaCl [11] and LiF [12]. Their average orientations indicated that the two planes (100) and (010) have been activated. Since the slip system for  $\sigma$  along  $\langle 111 \rangle$  is  $\{100\} \langle 011 \rangle$  with a Schmid factor  $f = 0.47$ , the ratio of critical resolved stresses for  $\{100\}$  and  $\{110\}$  slip planes is between 1.3 and 1.7 for  $T > 600$  °C ( $0.4 T_M$ ). At  $T < 600$  °C there is a rapid increase of the ratio, a situation similar to that of NaCl, KCl, KBr and KI where this increase occurs between 0.2 and 0.3  $T_M$  [11]. Although, NiO is much less ionic than alkali halides [4] and contains a fairly large amount of nickel vacancies [1], its plastic anisotropy seems to be dominated by the same mechanism as for ionic crystals.

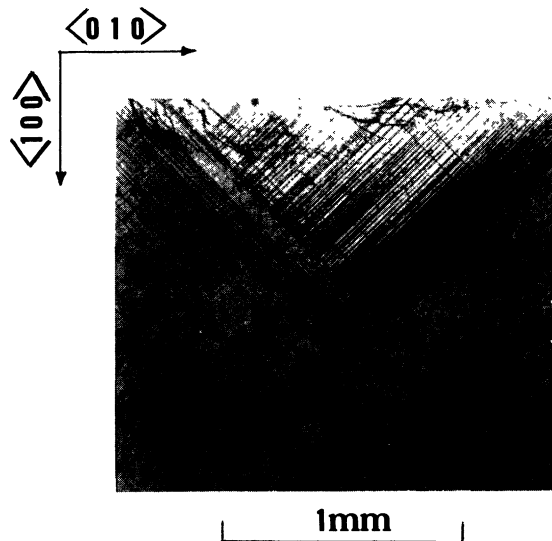


Fig. 4. — Chemical etch pits on a  $\{100\}$  face obtained by cleavage after deformation ( $T = 20$  °C,  $\varepsilon \sim 2.5\%$  under  $\sigma = 79$  MPa, parallel to  $\langle 100 \rangle$ ) of a Verneuil crystal. The surface is uniformly covered with etch pits except close to the compression face where glide bands can be distinguished.

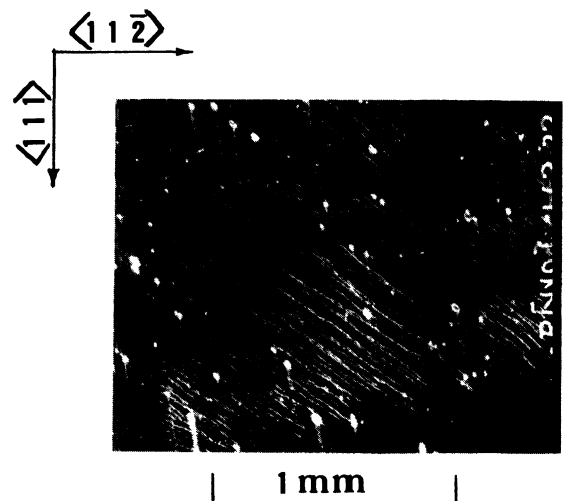


Fig. 5. — Slip steps in the  $\{110\}$  face of a Verneuil crystal deformed along  $\langle 111 \rangle$ ,  $T = 676$  °C,  $\varepsilon \sim 1\%$  under  $\sigma = 89$  MPa. The lines almost parallel to  $\langle 111 \rangle$  are polishing scratches.

**4.2. RATE CONTROLLING MECHANISM.** — The most striking result is that the plastic flow of NiO seems to be athermal between 0 and 600 °C; in this range almost all  $\sigma_{0.2}$  values fall between 50 and 70 MPa. A maximum may be detected around 400 °C (Fig. 2). Such an anomaly is a common observation in metals and alloys at low temperature [19]. In NiO, it may come from an unavoidable contribution of  $\theta$  which peaks at 400 °C (Fig. 3) or from residual impurities like Mn which gave a maximum of  $\sigma_{0.2}$  at 500 °C [3]. A similar behaviour is also associated to Portevin Lechatelier effect [10] which was not observed in our experiments.

In the following, we comment briefly about the obstacles to dislocation glide.

**4.2.1  $T < 190$  °C.** — In this temperature range,  $\sigma_{0.2}$  increases very quickly below 0 °C (Fig. 2) and  $V$  is in the range 20-40  $b^3$  at 77 K. This is typical of a Peierls mechanism which controls the glide of dislocations. Our data have been already analyzed by Skrotzki [13] together with results on ionic compounds. He found a Peierls stress  $\sigma = 330$  MPa for { 110 } slip and 1 320 MPa for { 100 } slip in NiO.

At room temperature, the curve  $\sigma_{0.2}$  vs.  $T$  reaches a plateau and  $V$  is of the order of a few 100  $b^3$ , independent of strain. This is typical of dislocation glide controlled by stable localized obstacles like impurities or forest dislocation [14], [11].

**4.2.2  $190 < T < 305$  °C.** — In this temperature range, the most prominent feature of the physical properties of NiO is the transition from antiferromagnetic to paramagnetic state ( $T_N = 250$  °C). Such a transition has been shown to influence the plasticity of CoO [6] and of NiO [3]. Our results on NiO (Fig. 2) indicate a smaller effect than the one previously reported. In the antiferromagnetic state, there is a doubling of the unit cell. When cooled through the Néel temperature a dislocation is associated to a magnetic stacking fault [15]; this has been observed by T.E.M. by many authors [16]. A moving dislocation increases the surface of the stacking fault; the additional energy  $\gamma$  per unit length of dislocation has to be provided by the mechanical work. Amelinckx [15] has suggested that  $\gamma \sim 1$  mJ/m<sup>2</sup>; with  $b = 0.296$  nm, the additional critical stress to move a dislocation is given by  $\tau = \gamma/b \sim 3$  MPa. This stress is much smaller than the flow stress of NiO (Figs. 1 and 2). This is an indication that magnetic domains, although pinned to dislocations, must have a limited influence on their motion. Many physical properties of NiO display

a discontinuity at  $T_N$  [1]. This is true, to some extent, for  $\sigma_{0.2}$  and  $\theta$  (Figs. 2 and 3). But, the most prominent feature is a trend for large  $V$  at small strains. We have no clear means to assign a magnetic origin to these observations.

Large work hardening rates as those reported in figure 3 are probably due to dislocation-dislocation interactions. For 1 000 <  $\theta$  < 2 000 MPa (Fig. 3), the values corrected for resolved stress and strain are between  $\mu/540$  and  $\mu/270$  ( $\mu =$  elastic, shear modulus) which are typical of multiple glide work hardening [20]. This is consistent with the existence of numerous dislocation reactions which have been observed in T.E.M. studies [7, 8]. Because of the high plastic anisotropy the product dislocations cannot move at  $T < 500$ -600 °C (Fig. 2) giving high  $\theta$  values (Fig. 3).

**4.2.3  $T > 362$  °C.** — In the high temperature range, two features appear to modify the description of plastic deformation of NiO: the plastic anisotropy almost disappears at 500-600 °C (Fig. 2) and recovery may become important as noticed in T.E.M. observations [8, 18]. This, very obviously, can be associated with the drop in  $\theta$  values (Fig. 3). At  $T > 1 200$  °C, it has been suggested that diffusion controlled recovery dominates the rate of plastic deformation of NiO [17]. However, at  $T \sim 1 000$  °C, creep data suggested that dislocation glide could have a part in the deformation process [17]. This is consistent with the large values for activation volume.

In this high temperature range, the obstacles to dislocation glide are dislocations, but these obstacles are easily overcome or eliminated by cross-slip or climb.

## 5. Conclusions and summary.

Bunsenite NiO can be deformed by compression at temperature down to 77 K. In these conditions, the overcoming of Peierls stress probably controls the kinetics of dislocation glide. At increasing temperatures, impurities or forest dislocations impede dislocation glide. The magnetic ordering which occurs below the Néel temperature does not seem to have a first order influence on plasticity contrary to what was previously published [3]. The mechanisms of plastic deformation of NiO in the various regimes could be better understood by a T.E.M. study which has still to be undertaken.

## References

- [1] *Basic properties of binary oxides*. Ed. by A. Dominguez-Rodriguez, J. Castaing and R. Marquez (Ediciones Univ. Sevilla) 1984.
- [2] DOMINGUEZ-RODRIGUEZ, A. and CASTAING, J., *Rad. Eff.* **75** (1983) 309.
- [3] DOMINGUEZ-RODRIGUEZ, A., CASTAING, J. and PHILIBERT, J., *Mat. Sci. Eng.* **27** (1977) 217.
- [4] CASTAING, J., *Ann. Phys.* **6** (1981) 195.
- [5] DOMINGUEZ-RODRIGUEZ, A. and CASTAING, J., *Revue Phys. Appl.* **11** (1976) 387.

- [6] CASTAING, J., SPENDEL, M., PHILIBERT, J., DOMINGUEZ-RODRIGUEZ, A. and MARQUEZ, R., *Revue Phys. Appl.* **15** (1980) 277.
- [7] MARUYAMA, S., GERVAIS, A. and PHILIBERT, J., *J. Mat. Sci.* **17** (1982) 2384.
- [8] FUERTES, M., Master of Science, Dpt. Met. and Mater. Sc. Case Western Reserve University, May 1980, Cleveland, Ohio.
- [9] DUBOIS, C., MONTY, C. and PHILIBERT, J., *Philos. Mag. A* **46** (1982) 419.
- [10] DOMINGUEZ-RODRIGUEZ, A. and CASTAING, J., *Script. Met.* **9** (1975) 551.
- [11] SKROTZKI, W. and HAASEN, P., *J. Physique Colloq.* **43** (1982) C3-119.
- [12] LIU, Z. G. and SKROTZKI, W., *Phys. Status Solidi (a)* **70** (1982) 433.
- [13] SKROTZKI, W. and SUZUKI, T., *Rad. Effects* **74** (1983) 315.
- [14] GROH, P., *Identification des mécanismes de déformation in : Dislocations et déformation plastique*, Ecole d'Été d'Yrivals (Ed. de Physique) 1979, p. 67.
- [15] AMELINCKX, S., *J. Physique Colloq.* **35** (1974) C7-1.
- [16] COATES, D. J., EVANS, J. W. and WESTMACOTT, K. H., *J. Mat. Sci.* **17** (1982) 3281.
- [17] CABRERA, J., DOMINGUEZ-RODRIGUEZ, A., MARQUEZ, R., CASTAING, J. and PHILIBERT, J., *Philos. Mag. A* **46** (1982) 397.
- [18] CADOZ, J., HOKIM, D., PELLISSIER, J. and VALLE, R., *J. Mat. Sci.* **17** (1982) 211.
- [19] PARKHOMENKO, T. A. and PUSTOVALOV, V. V., *Phys. Status Solidi (a)* **74** (1982) 11.
- [20] *Éléments de Métallurgie Physique* réunis par Y. Adda, J. M. Dupuy, J. Philibert, Y. Quéré, Tome 5 (La Documentation Française) 1979.
-